PROCEEDINGS OF SPIE

SPIEDigitalLibrary.org/conference-proceedings-of-spie

Preliminary design for the f/5 Nasmyth tertiary mirror configuration for the TSPM

María H. Pedrayes L., Joel Herrera V., Erika Sohn López-Forment, Fernando Quiros, Michael G. Richer, et al.

María H. Pedrayes L., Joel Herrera V., Erika Sohn López-Forment, Fernando Quiros, Michael G. Richer, J. Jesús González G., William H. Lee Alardin, "Preliminary design for the f/5 Nasmyth tertiary mirror configuration for the TSPM," Proc. SPIE 10700, Ground-based and Airborne Telescopes VII, 1070042 (6 July 2018); doi: 10.1117/12.2314377

SPIE.

Event: SPIE Astronomical Telescopes + Instrumentation, 2018, Austin, Texas, United States

Preliminary design for the f/5 Nasmyth tertiary mirror configuration for the TSPM

María H. Pedrayes L*[a], Joel Herrera V.[a], Erika Sohn López-Forment[b], Fernando Quiros[a], Michael G. Richer[a], J. Jesús González G.[b], William H. Lee Alardin[b].
[a] Instituto de Astronomía, Universidad Nacional Autónoma de México, sede Ensenada, B.C.
[b] Instituto de Astronomía, Universidad Nacional Autónoma de México, sede ciudad de México.

ABSTRACT

The preliminary design for the f/5 Nasmyth tertiary mirror opto-mechanical configuration for the 6.5m Telescopio San Pedro Mártir (TSPM), to be installed at the Observatorio Astronómico Nacional (OAN) in the Sierra San Pedro Mártir in Baja California is presented. The proposed system consists of support and alignment of the honeycomb mirror within the cell, the correction of the optical surface deformation, both tasks by means of an active push-pull pneumatic system and the correction of the displacements and rotations transferred by the Tube support structure to the configuration by means of electro-mechanical actuators. This optical configuration and four folded Cassegrain stations will be fully defined after first light of the f/5 Cassegrain configuration, so the requirements and considerations of these positions also need to be taken into account.

Keywords: tertiary mirror, TSPM, active push-pull system

1. INTRODUCTION

This work presents the preliminary design of the f/5 Nasmyth tertiary mirror opto-mechanical configuration for the 6.5m Telescopio San Pedro Mártir (TSPM) see Figure **1**-**1**, to be installed at the Observatorio Astronómico Nacional (OAN) in the Sierra San Pedro Mártir in Baja California. The objectives of this work are mainly four. The first is to obtain the preliminary design of a flat honeycomb-type elliptical mirror, implementing the specifications for the proposed f/5 Nasmyth optical configuration that will provide two operation modes: a spectroscopic telecentric mode and an imaging mode, both for 1° FOV.

The next objective is to introduce an active opto-mechanics system to dynamically compensate for the misalignment of the mirror in all the deformation range of the support structure, given by gravity, thermal and wind loads. The Nasmyth configuration and four folded Cassegrain stations will be fully defined after first light of the f/5 Cassegrain configuration, so the requirements and expected behavior at all these positions also need to be taken into account for the preliminary design stated in this work. The system proposed is based on one that already successfully operates at the 2.1m telescope at OAN.

The proposed system consists of a pull action implemented by vacuum pressure that holds the tertiary mirror and is a function of the zenithal angle. For that, a vacuum chamber is created through the back plate of the mirror and the inside walls of the mirror cell, with the aid of a hydrostatic ring that seals the chamber and also supports the mirror laterally. The push action that corrects the deformations of the optical surface, and aligns the mirror within the cell is implemented by means of 20 air bags with independent pressure and 3 linear actuators that act as hard points. The second task is to correct the displacements and rotations transferred by the telescope tube structure to the mirror by means of an active linear actuator system. This system consists of 3 units, which sense the inclination of the mirror with respect to the reference surface. The readings of the load cells allow the control system to correct the pressure in the bags, so that the load is kept within the proper range and the extra loads that correct the optical surface can be adjusted.

* pedrayes@astro.unam.mx; phone 011 5646 174-4580 ext 417; fax 011 5646 174-4607; http://www.astrosen.unam.mx.

Ground-based and Airborne Telescopes VII, edited by Heather K. Marshall, Jason Spyromilio, Proc. of SPIE Vol. 10700, 1070042 · © 2018 SPIE
CCC code: 0277-786X/18/$18 · doi: 10.1117/12.2314377

For the bag support and hydrostatic ring arrangement that correct the optical surface, several FEA analyses were performed, as well as analyses of the range of positive, vacuum and hydrostatic pressures, in order to determine the actuator range of displacements and the working loads for each load cells. The pneumatic components of the push-pull and the linear actuator system and its control are proposed. The third objective is to use the results of the deformations of the optical surface, obtained at several positions, for calculating the contribution of this mirror to the error budget. Finally, the preliminary design defines the interfaces and services need to be taken into account for the design of the rest of telescope. The coordinate systems used for the tube and M3 system are indicated in Figure 1-1 and Figure 2-1 left and right.

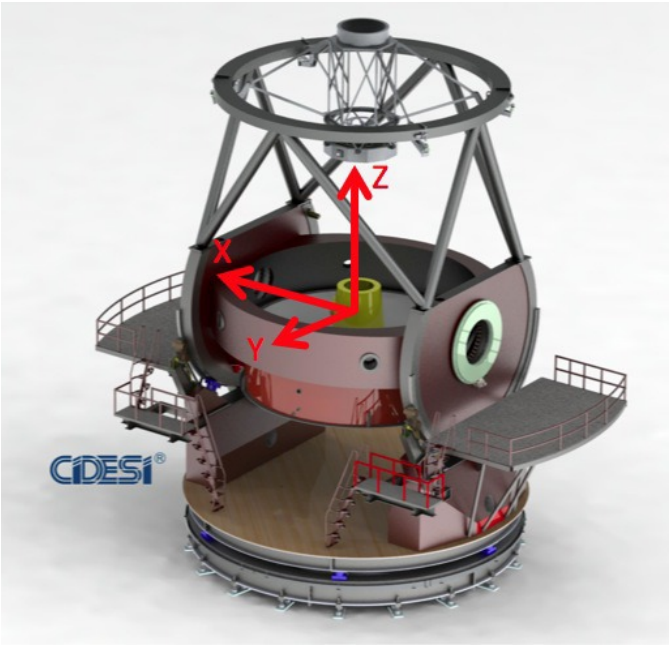

Figure 1-1. 6.5m Telescopio San Pedro Mártir (TSPM). Tube coordinate system

2. REQUIREMENTS

2.1 Optical parameters

Deviations allowed for the main optical elements of the telescope from their nominal position are described

Table 2-1.

The tertiary mirror alignment precision (including mounting tolerances and gravitational and thermal deformation at the nominal operational range) shall be equal or better than the given values.

Table 2-1. Optical deviation ranges of the main optical elements of the telescope TSPM.

Element	Dx (mm)	Dy (mm)	Dz (mm)	Tilt x (º)	Tilt y (º)
Primary	±1	±1	±1	±0.0083	±0.0083
Tertiary	-	-	±0.2	±0.006	±0.006
Barrel 2	±0.1	±0.1	±1	±0.0055	±0.0055
Rotator	±0.13	±0.13	±1	±0.0083	±0.0083

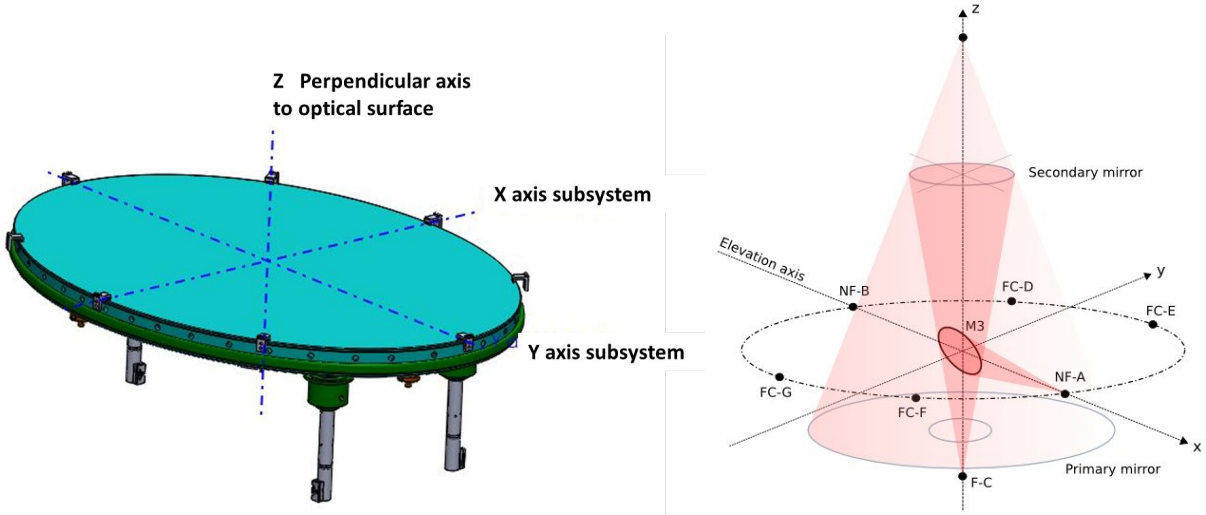

Figure 2-1. Left: Tertiary mirror subsystem coordinates. Right: Tertiary mirror and the folded focal stations.

The optical surface needed for the 1° field of view of the tertiary mirror in Nasmyth configuration for the TSPM [21] is a flat ellipsoidal surface with the dimensions of 2m in its mayor axis and 1.44 m in its minor axis. The deformations should be less than 600 X 10^{-9} m from peak to valley, that is, two fringes of irregularity in accordance with the requirements stated in [18].

2.2 Environmental Parameters

From the Telescope Specifications [20], the most important parameters considered for the subsystem are:

- Sustained wind speed limit: 50 km/h (13.9 m/s)
- Media wind speed: 13 km/h (4 m/s)
- Wind gusts speed limit: 70 km/h (19.4 m/s)
- Temperature range: -2°C to +18°C (goal: -5ºC to 18ºC)
- Temperature range degraded performance: -18°C to +30°C
- Temperature of reference: 6.8º C (for dimensions and tolerances, unless otherwise specified)
- Nominal day-night gradient less than 6 ºC.
- Nominal night temperature variation during the night is 0.5 ºC/hr.
- Nominal day temperature variation during the day is up to 2 ºC/hr.

The thermal sensibility of the tertiary mirror figure due to mount thermal effect shall be within these values.

2.3 Operational parameters

The M3 subsystem needs to rotate around the optical axis in 6 main positions to redirect the light coming from M2 to the different focal stations. These are the Nasmyth focal stations and the Folded Cassegrain Focal Stations. Considering the Telescope Tube Coordinate System the positions and nomenclature of each one of these stations are: Nas. A (0º), 65º (FC-E), 115º (FCD), Nas. B (180º), FC-G (245º), y FC-F (295º). Positive rotation is CW (clockwise), Figure 2-1.

Additionally the response of the subsystem to the movement of the Tube needs to be better than maximum elevation speed 0.8 °/s. [20].

3. CONFIGURATION

The main components of the Tertiary Mirror subsystem are: M3 mirror, M3 cell, M3 bag support, and the components needed to correct the deformations of the mirror within the cell due to its own weight and to compensate for the deformations of the system that supports it. These are a hydrostatic ring and an active system. The active system includes three linear actuators with load cells, an active push-pull system control and electro valves.

The components listed above are shown in Figure 3-1, Figure 3-2. The cell is the main support of the mirror. At the back face of the mirror are pads in contact that will transfer axial loads only via flexures to the load cells. The load-cell readings are fed to a control algorithm, which will define the position of the mirror with respect to a plane of reference, and with this information the active push pull system, positive pressurized bags and vacuum chamber, and the actuators for tip-tilting or focusing will be adjusted for the mirror to improve the quality of the surface or to correct its position with respect to the optical path (Figure 3-3, left and right). Each airbag with controlled-pressure will work as an independent force actuator (Figure **4**-**1** left).

The concept for correcting the optical surface deformations of the M3 mirror was taken from a newly developed configuration for the active mirror support system of the 2.1m telescope at the San Pedro Mártir Observatory [[5][6][7]]. To correct the displacements and rotations produced by the deformations of the mirror cell structure, a set of three electromechanical actuators was introduced. All the interfaces and components attached to the cell need to be airtight (low vacuum) since a vacuum chamber needs to be created between the back face of the mirror and the hydrostatic ring. For lateral passive support, a ring around the perimeter of the mirror with fluid will be used to produce a buoyancy force applied near the mirror's center of mass. This ring will have the function to diminish the effect of the flexural deformations produced by the lateral component of the mirror weight and it will be filled with API grade 1, oil with density of 10444 N/m3 or similar (Figure 3-2. Tertiary mirror subsystem.).

The tertiary mirror subsystem will be attached to the tertiary mirror tower with its transmission to position the mirror via spherolinders [9] (Figure 4-2). The tertiary tower system is not included in this work.

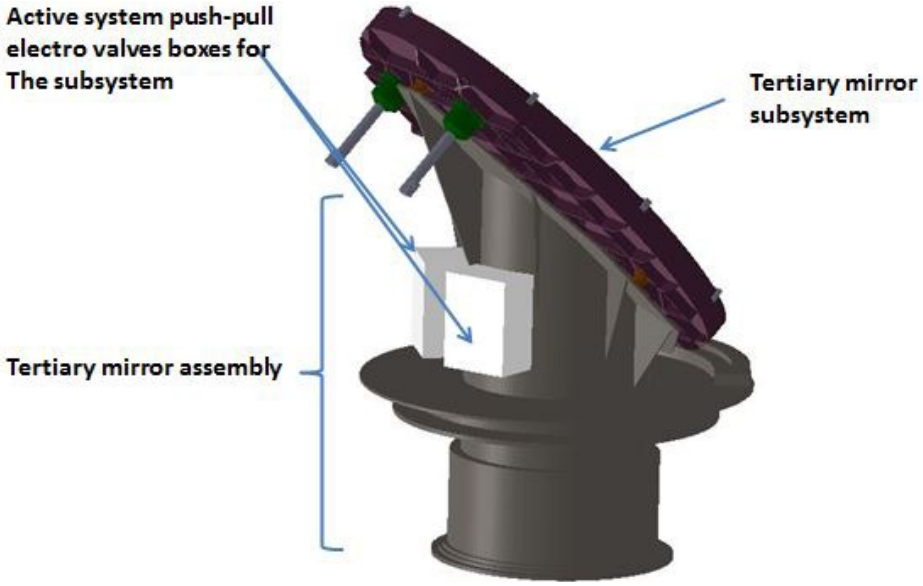

Figure 3-1. Subsystem attached to the assembly.

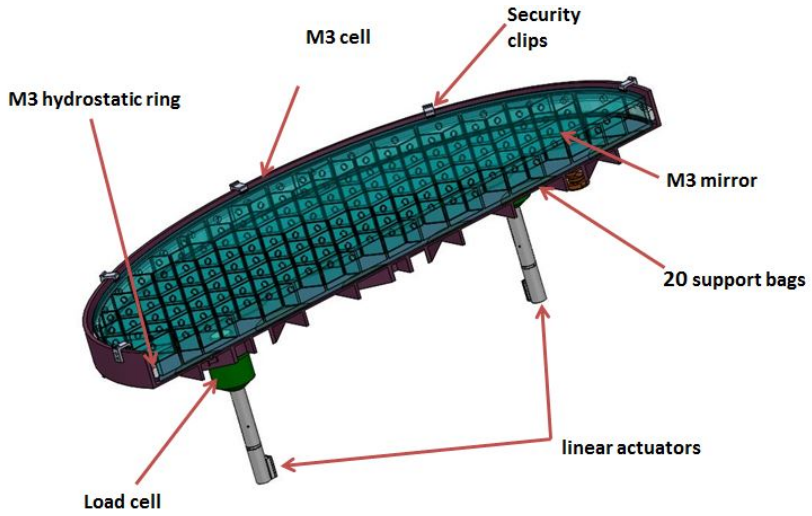

Figure 3-2. Tertiary mirror subsystem.

3.1 Active system

The principles here shown, as stated before, are based on the work developed at the Institute of Astronomy for the 2.1 primary mirror[5][6][7]. The algorithms are basically identical except for the adjustment needed for the response of the bags to produce the desired tip-tilt by means of the electromechanical actuators.

The active system consists of a push force produced by the air bags actuators that correct the deformation of the optical surface and a Pull Force Pv *A, induced by a homogeneous vacuum that is a function of the zenithal angle Z: (1 – cos(Z)), applied between the mirror cell and the back of the tertiary mirror with area A.

The push pressure in each airbag actuator consists of three terms, one to support the weight of the mirror, one to perform the desired deformations and a third term to correct the pressure based on the weight supported by each of the hard points, as follows[7]:

$$P_i = P_{wi}\cos(Z) + P_{di} + PID\left(\sum_j K_{ij}E_{pj}\right); i = 1 \dots 20, j = 1,2,3 \quad (1)$$

P_i = desired pressure in each airbag;
P_{wj} = pressure to support each portion of the mirror at zenith;
P_{di} = desired deformation pressure;
E_{pj} = error at each hard point (load cell);
PI D = proportional integral derivative algorithm that corrects the pressure based on the error at each hard point and a propagation function *K i,j*.

The propagation function has been taken to be a plane defined by the error at each hard point, evaluated at the position of the bags, and weighted by the portion of mirror that each bag supports $(P_{wi})(M_{tot})$. In this manner, an uneven error of support at the hard points results in a pressure change at the actuators that tilts the mirror as a rigid body. The error at each hard point, in turn, has the following form:

$$\mathrm{E_{pj}} = \mathrm{M_j^c} - \left(\mathrm{P_{w_j^c}}\cos(\mathrm{z}) + \mathrm{P_{d_j^c}}\right); \mathrm{j} = 1,2,3 \quad (2)$$

$\mathrm{M_j}$ = measured force on a load cell
$\mathrm{P_{w_j^c}}$ = calculated weight that a cell should be standing,
$\mathrm{P_{d_j^c}}$= desired deformation at the position of the hard points (cell-actuator).

The control system monitors the pressure at each airbag actuator *(Mi),* and provides a proportional correction to reach the desired pressure *Pi.* The pull force is introduced in order for the actuator airbags to feel a constant force equivalent to the mirror weight that is independent of Z (vacuum) the equation is applied [5]:

$$P_b^i = P_w \cos(Z) + P_d^i - P_v(1 - \cos(Z)) = Pw + P_d^i \quad (3)$$

$$P_v = -P_w \quad (4)$$

$P_b^i =$ actuator pressure of each bag

$P_w =$ pressure due to mirror weight $= -P_v$

$P_d^i =$ pressure neede to produce the desire deformation

P, has to be equal to minus the total mirror weight divided by its total area, in order for the cos(Z) terms to cancel out. The final effect is still the equivalent of the telescope always pointing at the zenith.

3.1.1 Linear actuators system

The linear actuators are introduced to compensate for the misalignment of the optical components from the optical axis given by the deflections of the interface with the mirror tower as well as from the Tube structure (Figure 3-2, Figure 3-3). The actuators proposed are 3. They will be located in line with the load cells and as they move in the axial direction the readings of the load cells will cause the control system to adjust the pressure in the bags so the load sensed is kept in the proper range so the extra loads that deform the optical surface of the mirror can be adjusted. This configuration needs to be airtight so the vacuum chamber can be formed.

For the actuators to rotate the mirror in a tip tilt mode, a combination of a spatial rotation and translation needs to be applied, because the origin of the optical surface is not in the same plane than the actuators. If a displacement in the Z direction needs to be applied to the mirror these combinations are not needed. So the actuators are:

$$p_0\colon (0\ ,0\ ,0)(origin\ at\ the\ mirror),$$
$$p_1\colon (x_1\ , y_1\ , -z_0 + \delta_1),\ p_2\colon (x_2\ , y_2\ , -z_0 + \delta_2),\ p_3\colon (x_3\ , y_3\ , -z_0 + \delta_3), \quad (5)$$

$-z_0$ is the distance from the optical plane where the tip of the actuator is located and is the displacement each actuator needs to apply.

The equations for displacement (extension or contraction) $\delta_{\#}$ that need to be applied by each actuator to obtain the tip-tilt are:

$$\begin{aligned}
\delta z_1 &= -x_1 \cos(\alpha)\sin(\beta) - y_1 \sin(\alpha) + z_o\,[1 - \cos(\alpha)\cos(\beta)],\\
\delta z_2 &= -x_2 \cos(\alpha)\sin(\beta) - y_2 \sin(\alpha) + z_o\,[1 - \cos(\alpha)\cos(\beta)],\\
\delta z_3 &= -x_3 \cos(\alpha)\sin(\beta) - y_3 \sin(\alpha) + z_o\,[1 - \cos(\alpha)\cos(\beta)]
\end{aligned} \quad (6)$$

α and β are orthogonal angles. The α angle is a rotation with respect to the x-axis (i.e. a rotation in the y-z plane in the sense of going from the z to the y axis). The β angle is a rotation with respect to the y-axis (i.e. a rotation in the x-z plane in the sense of going from the z to the x axis).

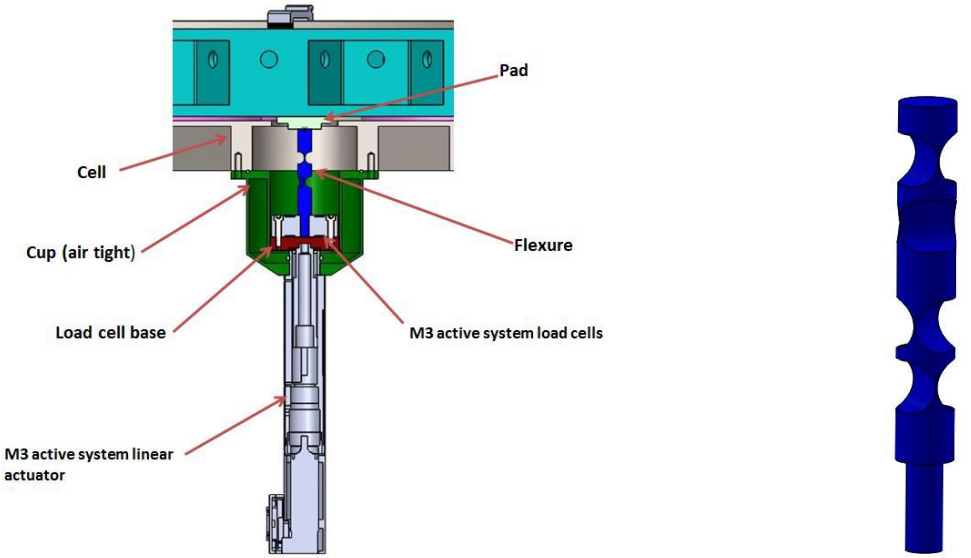

Figure 3-3. Right: Linear actuator with load cell, flexure and pad [14][15][13] . Left: Flexure.

3.4.3 Push-Pull system

In Figure 3-4, the main components of the push-pull system are presented. The components for the airbag actuators tertiary subsystem are enclosed in the right side box of the diagram. This system consists of 20 flat airbags distributed over the area of the ellipse (Figure 4-1). The pressure in each bag is given by the quantity of air that is injected or extracted by the electro valves. There is a damper in each airbag supply line that filters the pulses that can be generated by the electro valves. Also each line includes a pressure sensor. The air that goes to the electro valves comes from a reservoir that is included in the control box of the actuators so a constant pressure is guarantee. The air that is extracted from the bags by the electro valves goes to a vacuum reservoir that will be located at one of the tripods. This system will also include the control for the actuators and the load cells.

The components for the vacuum chamber for the tertiary subsystem are enclosed in the left and middle boxes and it includes one push electro valve, one pull electro valve, a damper that also has the function to filter the pulses that can be generated by the electro valves, the control of an electronic pressure sensor for the vacuum in the cell and an electro valve that punctures the positive pressure reservoir as a security measure to protect the mirror from damage.

The positive pressure in the air bags needs to be regulated with high precision at least 7 Pa (0.001 psi) in order to obtain the resolution needed for the optical surface to be corrected. The maximum flow rate that is expected for the vacuum is of the order of 11 l/s, which is faster than the telescope's pointing speed. The control cycle time was adjusted to 100 10^{-3}s. , which is fast enough to handle the telescope's 0.8 °/s. pointing movements. The boxes that will hold the pneumatic components and the electronic control need to be thermally controlled by means of an extraction line. The description of the control architecture will be addressed in chapter 7.

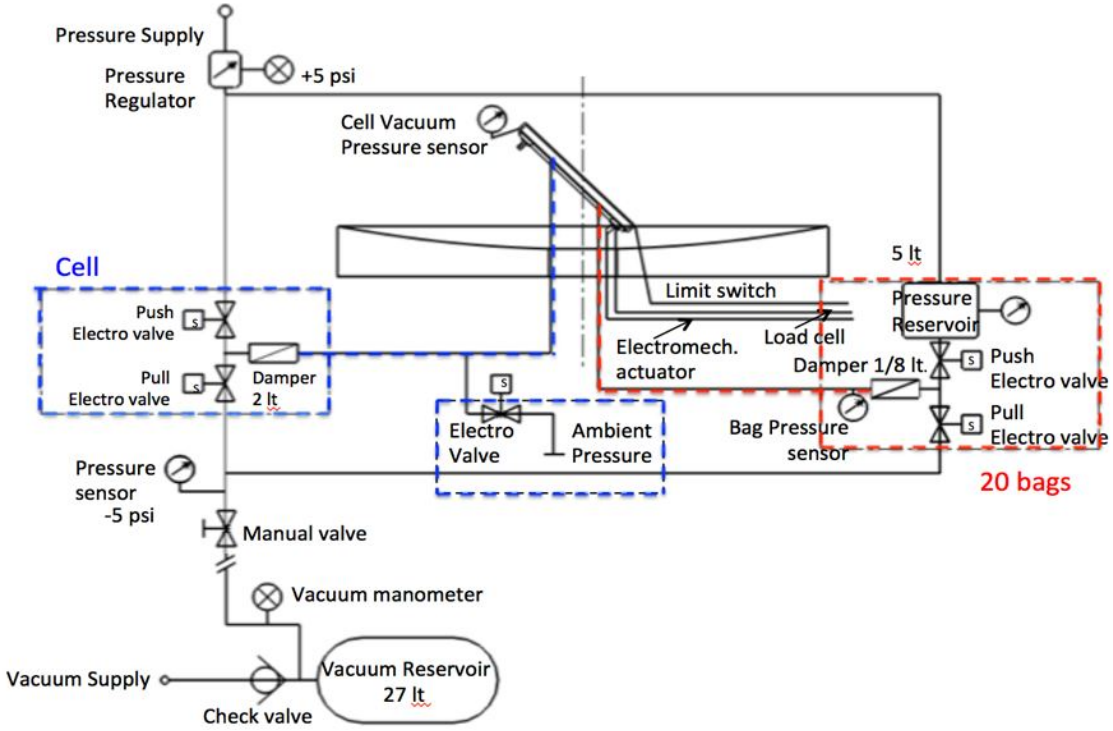

Figure 3-4. TSPM general block diagram of the push-pull pneumatic system.

4. COMPONENTS DESIGN

4.1 Tertiary mirror

The departure idea was to evaluate the Magellan mirror and support configuration[2][3], GTM tertiary mirror configuration[4] as well as the active support system of the 2.1m Telescope at San Pedro Mártir Observatory[5][6][7] and then obtain the tertiary mirror TSPM configuration. The Magellan mirror is of the honeycomb type with holes in the ribs for thermalisation. The 2.1m. mirror is a thick meniscus which is very heavy since it is an old telescope, so the honeycomb structure was chosen for this mirror.

A honeycomb structure type was chosen for the M3 because of its high stiffness – to – weight ratio obtaining a light-weighted mirror. The main dimensions of the optical surface were determined by the field of view required at the Nasmyth focal station [21][18]. To obtain the remaining parameters of the tertiary flat ellipsoidal mirror with a flexural rigidity D[1] similar to the one of the Magellan mirror, but with the required dimensions, calculations were made with the results shown next, using the formulas given text books[1][8]. The dimensions of the Magellan mirror were taken from the electronic drawing [3]. The front and back plates of the mirror were defined with the same thickness as in the original mirror.

To obtain the flexural rigidity [1], first it is needed establish the values of the face sheet thickness, the rib height, the rib solidity ratio for then to obtain the equivalent bending thickness and with the material properties of the mirror the flexural rigidity can be calculated. The parameters that can vary to obtain the rib solidity are the rib height and rib thickness, the face sheet thickness and the inside diameter of the internal cell. The lower the solidity ratio, the greater the stiffness.

In order to maintain the same flexural rigidity of the Magellan, the only parameter that was modified to obtain the rib solidity ratio is the diameter B of the inside cell [1]. The total thickness of the honeycomb mirror for the TSPM was

established to be the same as in the Magellan. With the rib solidity ratio we calculate the remaining parameters of the honeycomb mirror optimizing it's weight. See drawing [10] for the dimensions.

The material selected is the titanium silicate glass ULE from Corning [16] .It is the same as Magellan because it's known thermal properties and it's low mass density. The calculations made to obtain the parameters for the M3 of the Magellan and then the M3 for the TSPM are:

```
ClearAll;
tw = 0.005; (*rib thickness*)
B = 0.103; (*inscribed circle diameter*)
η = ((2 B + tw) tw) / (B + tw)^2 (*rib solidity ratio*)
tf = 0.013; (*face sheet thicknes*)
a = 1.09 / 2;
b = 0.766 / 2;
A = π x a x b; (*area of the mirror*)
h = (a - b)^2 / (a + b)^2;
Circunf = π (a + b) (1 + (3 h / (10 + √(4 - 3 h))));
c = Circunf x 0.010;
hc = 0.0732; (*rib height*)
ρ = 2.20 x 10^3; (*ULE density*)
bb = 0.062; (* hole diam*)
ww = 6 (π (bb / 2)^2) x tf;
W = ρ x A (2 x tf + η x hc) - ww + ρ x c x hc (*aprox weight without periferical flanges*)

0.0904492
```

MAGELLAN 51.7918

The mass obtained in the calculations is almost the same as the value of 58 kg that appears in the electronic drawing [3].

```
In[1]:= ClearAll;
        tw = 0.006;
        B = 0.123;
        η = ((2 B + tw) tw) / (B + tw)^2
        tf = 0.013;
        a = 2.000 / 2;
        b = 1.440 / 2;
        A = π x a x b;
        h = (a - b)^2 / (a + b)^2;
        Circunf = π (a + b) (1 + (3 h / (10 + √(4 - 3 h)))); (*Ramanujan aproximatio
        c = Circunf x 0.010;
        hc = 0.0732; (*rib height*)
        ρ = 2.20 x 10^3; (*ULE density*)
        bb = 0.062;
        ww = 6 (π (bb / 2)^2) x tf (*vol aujeros*);
        W = ρ x A (2 x tf + η x hc) - ww + c x hc x ρ
Out[4]= 0.0908599
```

TSPM. Out[16]= 171.24

The final parameters and dimensions obtained are: major axis = 2.000 m, minor axis = 1.440 m, total thickness = 0.100 m. The frontal and back plates have the same thickness of 0.013 m.
The mass properties of the mirror are: density = 2210.00 kg / m^3, mass = 171.209 kg, volume = 0.077 m^3
Total Surface area = 13.429 m^2. Area of the each main surface of the mirror= 2.266 m^2
Center of mass: X = 0.000 m., Y = 0.000 m., Z = -0.052 m..

See the electronic drawing of the tertiary mirror for the TSPM [10] for more information.

4.2 Bag Support arrangement

The air bags consist of 20 identical and independent flat pneumatic actuators. They work with positive pressure. The dimension of each is 0.230 m in ϕ, with an area of 0.0415475628 m^2. The area covered by the bags is 0.8309 m^2, which is approximately 37 % of the total area of the mirror's back plane [13].

The 22 gr. airbags can be inflated to a maximum volume of 41 ml. The material proposed for the bags is 330 D. Cordura Nylon, polyurethane-coated fabric [17] with more flexible materials than standard Cordura fabrics.

The dimension and distribution of the arrangement was determined from several FEA analyses made to obtain the best response, given that the shape of the mirror does not allow a symmetrical distribution if one considers that the actuators need to work against the ribs not the pockets of the honeycomb. Additionally, the perimeter rib of the mirror weighs more than the ribs at the center of it. Regardless of these considerations, the results obtained with the selected distribution gave good results as will be shown later.

The idea of using large area supports is that deformations are produced by shear forces at the position of the supports. These can increase the mean bending deformations by a factor of two, but are reduced substantially when the size of the supporting airbag actuator is increased [13]. The final distribution is shown in the left Figure **4**-**1**.

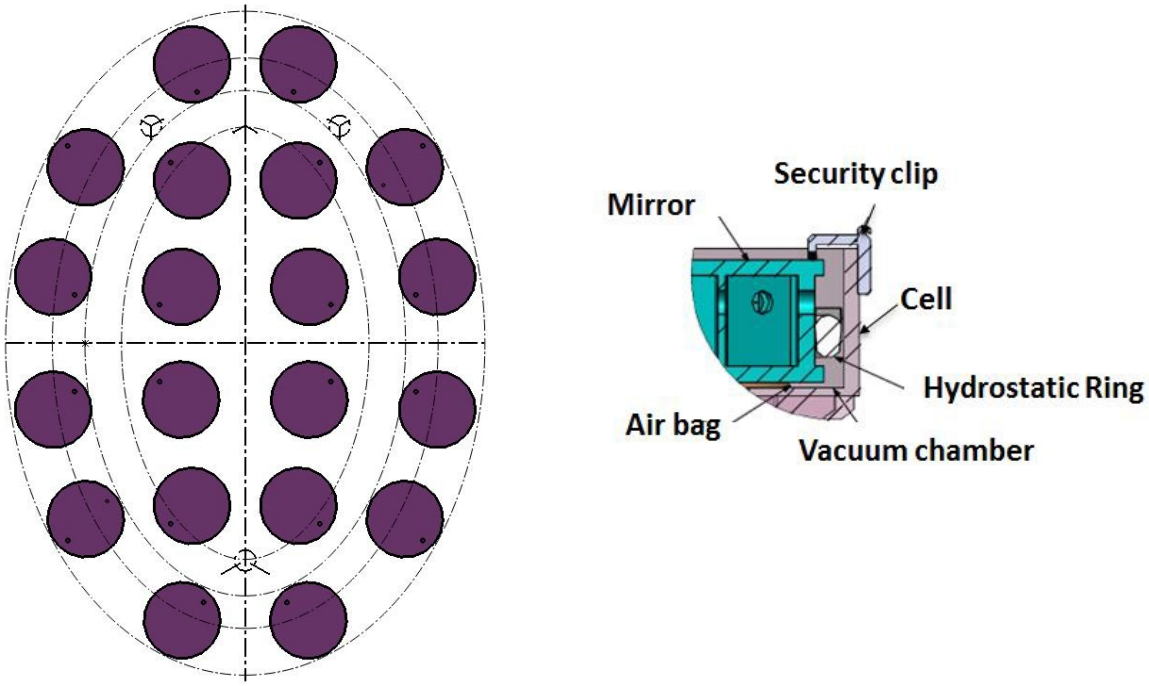

Figure 4-1. Left. Positive pressurized bags arrangement. Right, Profile of hydrostatic ring.

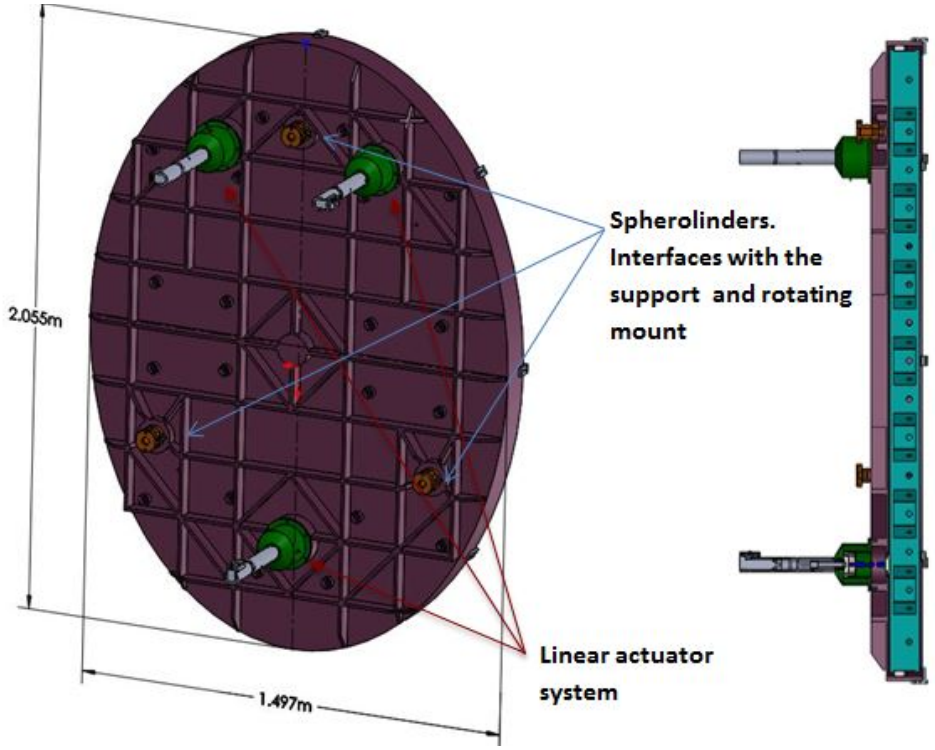

Figure 4-2. Back and section view of the cell with the description of the main interfaces [11][12][9].

5. STATIC STRESS ANALYSIS OF THE SUBSYSTEM.

Flexural deformations of the optical surface and the support cell were obtained with FEA taking into account all the considerations described, as the design of the sandwich/honeycomb mirror, distribution, size, material and pressures for each bag, hydrostatic ring position and fluid density, actuators/load cell position, stiffness and area of action at the back of the mirror. The coordinate used system used is the tertiary mirror coordinate system.

All the elements that work on the mirror to correct the optical surface deformation, as well as to compensate for the deviation from the optical path produced by the deflections of the telescope Tube, were simulated in the FEA analysis: The action of each load cell with the actuator in the mirror were simulated by 3 zones with 24 springs each to work perpendicular to the back surface of the mirror with a stiffness given by the load cell, with no restriction in X Y to allow for tip-tilt in the flexor attached to each load cell. The stiffness given is $K = 90.677 \times 10^6$ N/m.

The hydrostatic ring was simulated with hydrostatic pressure applied at the lateral surfaces of the mirror and cell where this ring will be in contact. 4 springs are located at the main axis of the mirror to give stability to the model with stiffness of $K = 8 \times 10^4$ N/m. Each spring restricts the movement in X-Y. 73 boundary conditions at the back of the cell restrict its movement in XYZ and are applied at the three zones where the interfaces with the tertiary tower will be located.

5.1 Results of the optical surface

The analyses were made varying the orientation of the gravity vector, also the surface pressure loads of each bag, the vacuum between the back surface of the mirror and the cell and the hydrostatic pressure vector. From the working range

of the telescope, the positions where the gravity affects the most are presented. The coordinates used to present the results are the subsystem coordinates in accordance with the reference [19]. The results of the displacements of the optical surface are summarized in the following tables.

In Table 5-1 the forces introduced are gravity, positive and vacuum pressure.

Table 5-1. Mirror with push-pull, hydrostatic and gravity loads.

		Displacement Range Units in meters			
F Station	T Orient.	X	Y	Z	Magnitude
Nas. B	Zenith 90°	0.2e-6 to -0.2e-6	0.3e-6 to -0.1e-6	-2e-9 to -9e-8	0.3e-6 to 5e-8
	45°	641e-6 to 604e-6	422e-6 to 449e-6	6e-9 to -0.1e-6	777 e-6 to 743e-6
	15°	15e-6 to 14e-6	-71e-6 to -71e-6	5e-9 to -0.2e-6	73e-6 to 72e-6

In Table **5-2** the values given are the results of the same forces introduced in the analysis made before plus the thermal load of -18 °C (with a stress-free reference temperature of 6.8 °C, which is the minimum temperature for observations with degraded performance). These values need to be added to the error budget to obtain the final range of displacement for the actuator.

Table 5-2. Mirror with push-pull, hydrostatic, thermal and gravity loads.

		Displacement Range Units in meters			
F Station	T Orient	*X*	Y	Z	Magnitude
Nas. B	Zenith 90°	0.5e-6 to -0.5e-6	0.8e-6 to -0.6e-6	3e-6 to -7e-6	7e-6 to 2e-8
	45°	64e-6 to 60e-6	-42e-6 to 45e-6	2e-6 to -5e-6	77e-6 to 74e-6
	15°	144e-6 to 141e-6	-710e-6 to -713e-6	7e-7 to -2e-6	727e-6 to 720e-6

In all of the analyses made to the mirror the Maximum Principal Stresses in tension were below to 0.2 M Pa, compared to the 20 MPa value given in[[8], pg. 272], the maximum value is 100 times less than the recommended limit. At the position where the pads of the linear actuators are going to be located the reactions obtained gave us the load that the cells will be sensing and they will be from 52 to 17 N. These forces are only produced by the correction of the optical surface but not for the active compensation of the misalignment of the optical components. The forces expected to focus or tip-tilt the mirror will be around this order of magnitude. The pressure range obtained in the individual bags goes from 1045 Pa up to 2200 Pa.

The RMS results of the optical surface of each analysis are presented in Table **5-3**. The contribution of the error produced by the deformation of the M3 is less than 0.04% of the total degradation of the image. This means 0.011arc sec FWHM, which has no weight over the total error budget.

Table 5-3. Deformations of the optical surface of the mirror at different positions.

Mirror pointing at focal station	Tube	RMS deformation normal
orientation to Nas. A	Zenith 90°	42
orientation to Nas. B	45°	37
orientation to Nas. B	15°	50

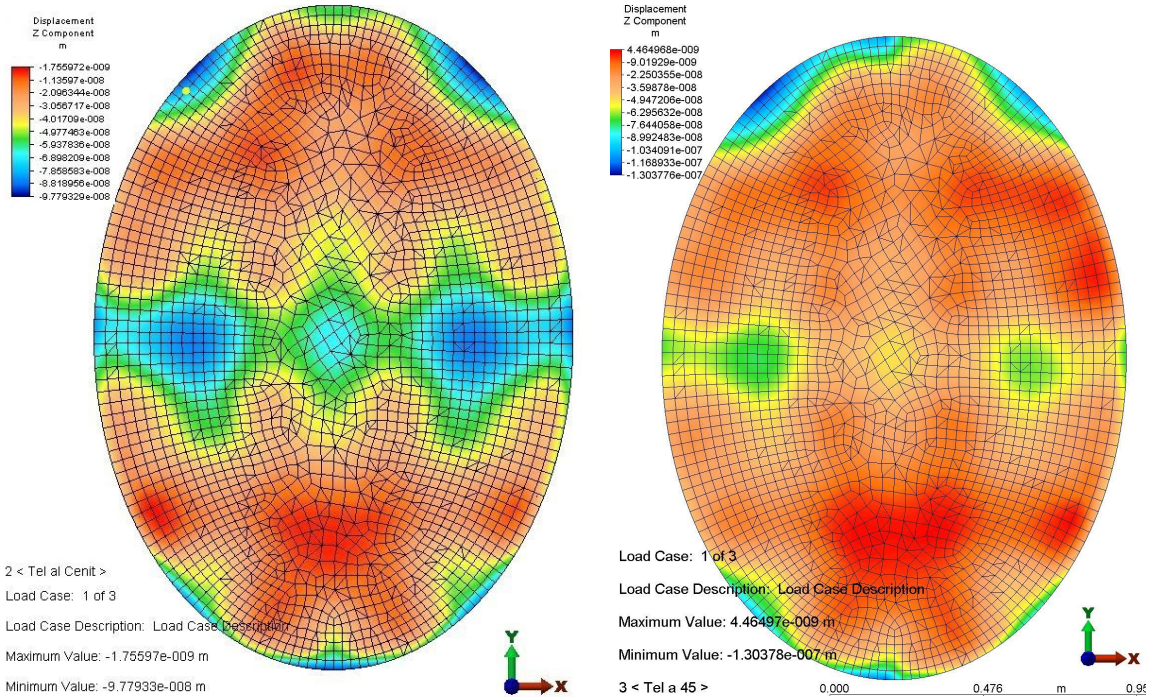

Figure 5-1. . Left: Optical surface when the system is pointing towards Nasmyth A, focus and Tube is pointing Zenith. Right: optical surface when M3 Subsystem is pointing at Nasmyth B, focus and Tube is pointing at 45 ° from horizon.

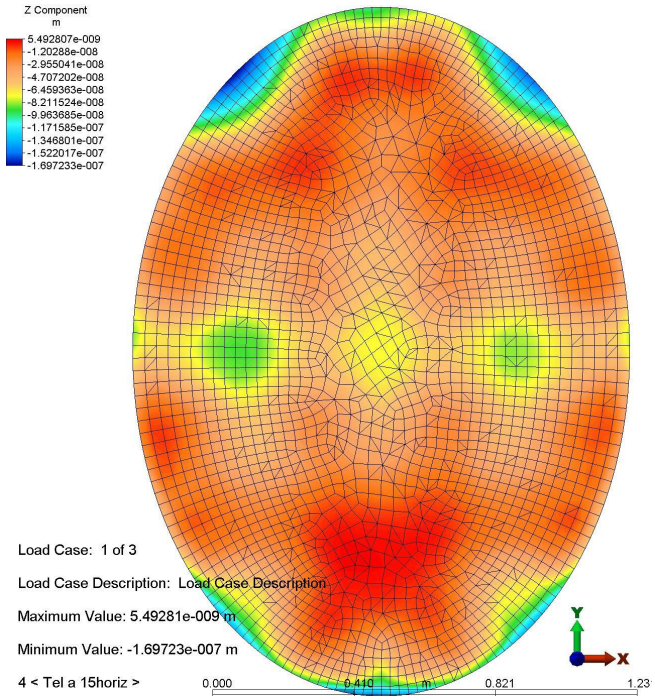

Figure 5-2. Optical surface when M3 Subsystem is pointing at Nas B focus and Tube is pointing at 15 ° from horizon.

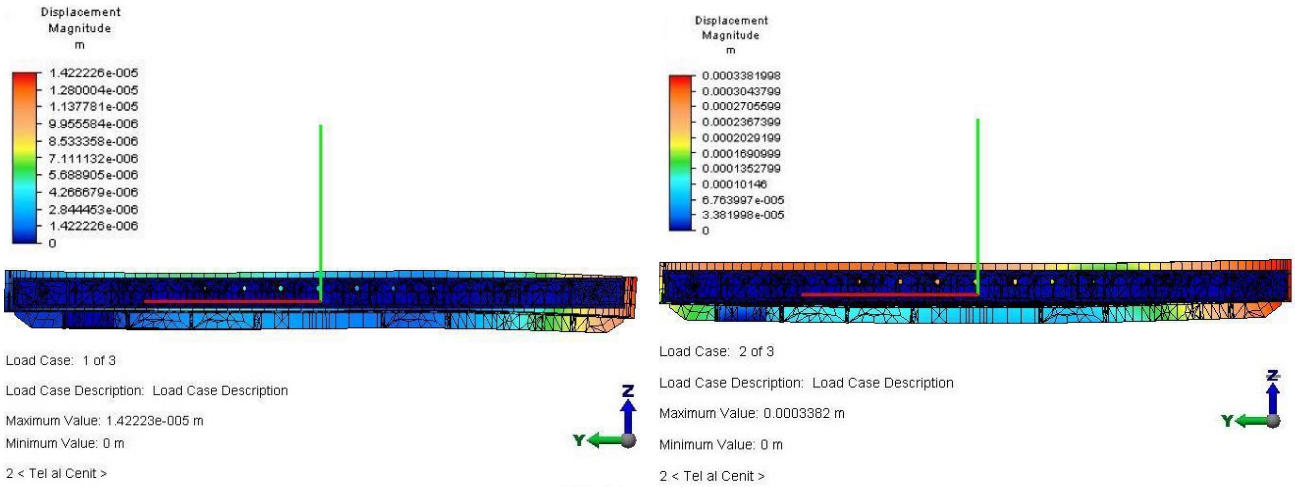

Figure 5-3. Tertiary subsystem. Left image with only gravity load. Right image with gravity, pressures and thermal loads.

6. GENERAL ASSEMBLY

6.1 Mass of the subsystem

The mass properties for the subsystem, without the control boxes and the connectors and hoses, given in the Tube coordinates system is: mass = 501.28 kg. Center of mass with respect to the optical surface (where the coordinates for the subsystem are) is: X = 0.00, Y = -0.13, Z = -0.02. Total mass is given in Table 6-1. Mass of tertiary mirror subsystem

Table 6-1. Mass of tertiary mirror subsystem

Components	Mass Kg.
Cell	298.28
Mirror	171.20
Bags + relief valves + connectors and hoses	10.00
Hydrostatic Ring	8.00
3 Spherolinder interfaces	5.52
3 Active Systems	16.8
Control Boxes	40.0
Total	549.8

6.2 Modal Analysis

Table 6-2. Tertiary Mirror subsystem frequencies**.**

Mode	Frequencies (Hz)
1	139.78
2	152.45
3	201.23
4	289.32
5	346.94
6	350.54
7	357.19
8	374.32

The first 5 are mainly given by the cell. The first natural frequency of the mirror alone is 224.52 Hz. The first natural frequency of the cell is 123.165 Hz.

6.3 Linear actuator performance

The traveling distance and resolution needed for the actuators is determined mainly by the optical deviation ranges of the main optical elements allowed for the TSPM telescope. First the maximum deviations given in Table 2-1 are considered.

Then the position of the actuator unit is also taken in account (Figure **4**-**2**). The coordinates given are of the pads that are in line with the actuators and form one unit (Figure 3-3). These pads are in contact with the back of the mirror so the coordinate Z_o is the mirror total thickness. So from the positions of the actuator with respect to the origin of the coordinate system and the deviation allowed for the tip-tilt calculations are made to obtain the total traveling range. See Equation **6**-**1** Equation **6**-**2**.

Next FEA static and thermal analyses of the tertiary mirror subsystem attached to the tower system (Figure **6**-**1**) were made to obtain an approximation of the maximum travel the actuators will need to compensate for the flexures and tilts produced by the gravity and thermal loads on the system support structure at the significant positions in altitude of the Tube and the tertiary system in 3 focal stations, this in order to align the optical surface of the mirror to the optical axis of the telescope. In this model the mirror was simulated with nodal masses and the location of the actuators with rigid elements of K=1e4 N/m with translation degree of freedom. The tertiary tower was fixed at the base.

```
In[27]:= ClearAll; (*dimensions are in meters*)
         x1 = -0.283433;
         y1 = 0.654531;
         x2 = 0.283433;
         y2 = 0.654531;
         x3 = 0;
         y3 = -0.6544874;
         zo = 0.100280;
         α = 0.006 Degree;
         β = 0 Degree;
```

Equation 6-1

```
In[37]:= δz1 = -x1 Cos[α] Sin[β] - y1 Sin[α] + zo (1 - Cos[α] Cos[β])
         δz2 = -x2 Cos[α] Sin[β] - y2 Sin[α] + zo (1 - Cos[α] Cos[β])
         δz3 = -x3 Cos[α] Sin[β] - y3 Sin[α] + zo (1 - Cos[α] Cos[β])

Out[37]= -0.0000685418

Out[38]= -0.0000685418

Out[39]= 0.0000685383
```

```
In[14]:= ClearAll; (*dimensions are in meters*)
         x1 = -0.283433;
         y1 = 0.654531;
         x2 = 0.283433;
         y2 = 0.654531;
         x3 = 0;
         y3 = -0.6544874;
         zo = 0.100280;
         α = 0 Degree;
         β = 0.006 Degree;
```

Equation 6-2

```
In[24]:= δz1 = -x1 Cos[α] Sin[β] - y1 Sin[α] + zo (1 - Cos[α] Cos[β])
         δz2 = -x2 Cos[α] Sin[β] - y2 Sin[α] + zo (1 - Cos[α] Cos[β])
         δz3 = -x3 Cos[α] Sin[β] - y3 Sin[α] + zo (1 - Cos[α] Cos[β])

Out[24]= 0.0000296816

Out[25]= -0.0000296805

Out[26]= 5.49847 × 10^-10
```

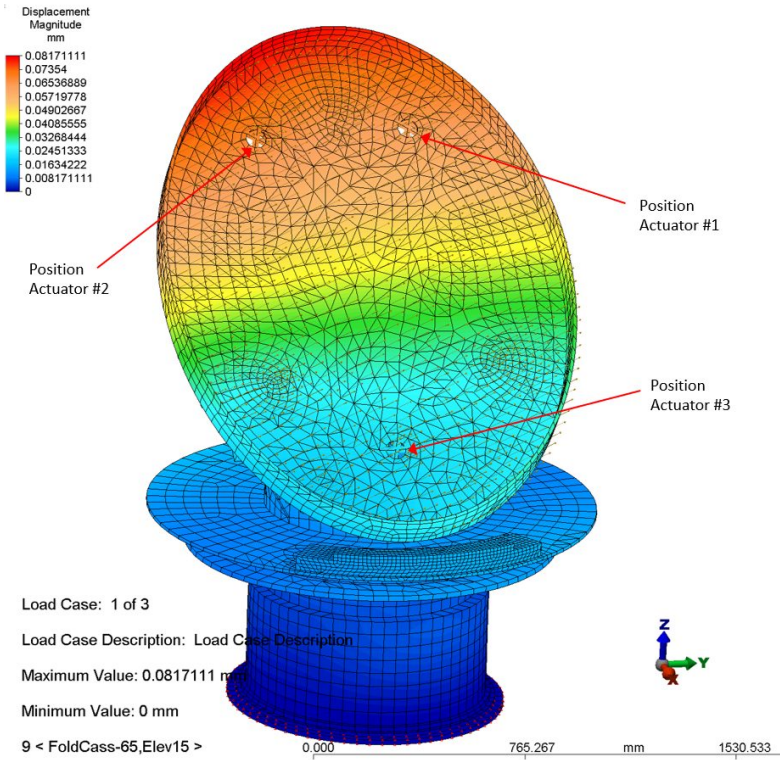

Figure 6-1. Position of the actuators in the FEA model where the tower system is oriented at FC F, elevation at 15°.

The thermal load applied was -18 °C (with a stress-free reference temperature of 6.8 °C), which is the minimum temperature for observations with degraded performance. As can been seen in Table **6**-**3** after transformation of coordinates to the tertiary mirror subsystem, the maximum actuators range is mostly determined by the flexures produced by the minimum thermal load on the structure.

If we compare the results of the tip-tilt calculations given by the values establish in the Figure **3**-**1** with the ones obtained with the FEA analyses without temperature the displacements are in the established range, but the Z displacement that the actuators need to compensate for the thermal deformations is approximately 0.350 mm compare to the 0.2 established. Up to these values obtained in the analyses and with the configuration presented in this work, the deformations and misalignments can be compensated.

For the range of travel and resolution needed the M-238.5PG High- Load Linear Actuators from PI [15] were chosen, but a modification needs to be made because working temperature range and it's dimensions. We need no more than 3 mm of travel, also the operating temperature range is above than we need of -18 to 30 °C. Another actuator could be used, namely N-216.20 NEXLINE® Piezo Stepping High- Load Actuator, with 20 mm of travel range and 600 N push pull force but it has the same operating temperature problem. So, pending work is to confirm the operating range of the mentioned actuator and/or search other candidates.

Table 6-3. FEA analyses of tertiary subsystem attached to the tower to determine max. actuators travel range.

Telescope			Actuator Travel Range in mm		
F. Station	Tube Orientation	Temp °C	1	2	3
Nas A	90º	6.8	0.018	0.019	0.008
		-18	0.099	0.099	0.088
Nas A	0º	6.8	-0.008	0.008	0.000
		-18	0.284	0.300	0.292
FC-E	45°	6.8	-0.030	-0.025	0.003
		-18	0.344	0.348	0.301
FC-E	15°	6.8	-0.053	-0.047	-0.002
		-18	0.239	0.246	0.290
FC-F	45°	6.8	0.051	0.055	0.008
		-18	0.344	0.348	0.301
FC-F	15°	6.8	0.056	0.063	0.006
		-18	0.349	0.355	0.298

7. CONTROL ARCHITECTURE

The control of the subsystem is divided into 3 main interlaced blocks: load cell control, pressure readings and electro valves control. The distribution of the control architecture allows for an orderly integration and growth of the systems, but keeping only a few common standards like is the case of the communication standard. The EtherNet/IP communication modules are proposed to reduce the wiring and to arrange the sensors in buses/ducts. The block system diagram proposed is shown in Figure **7**-**1**.

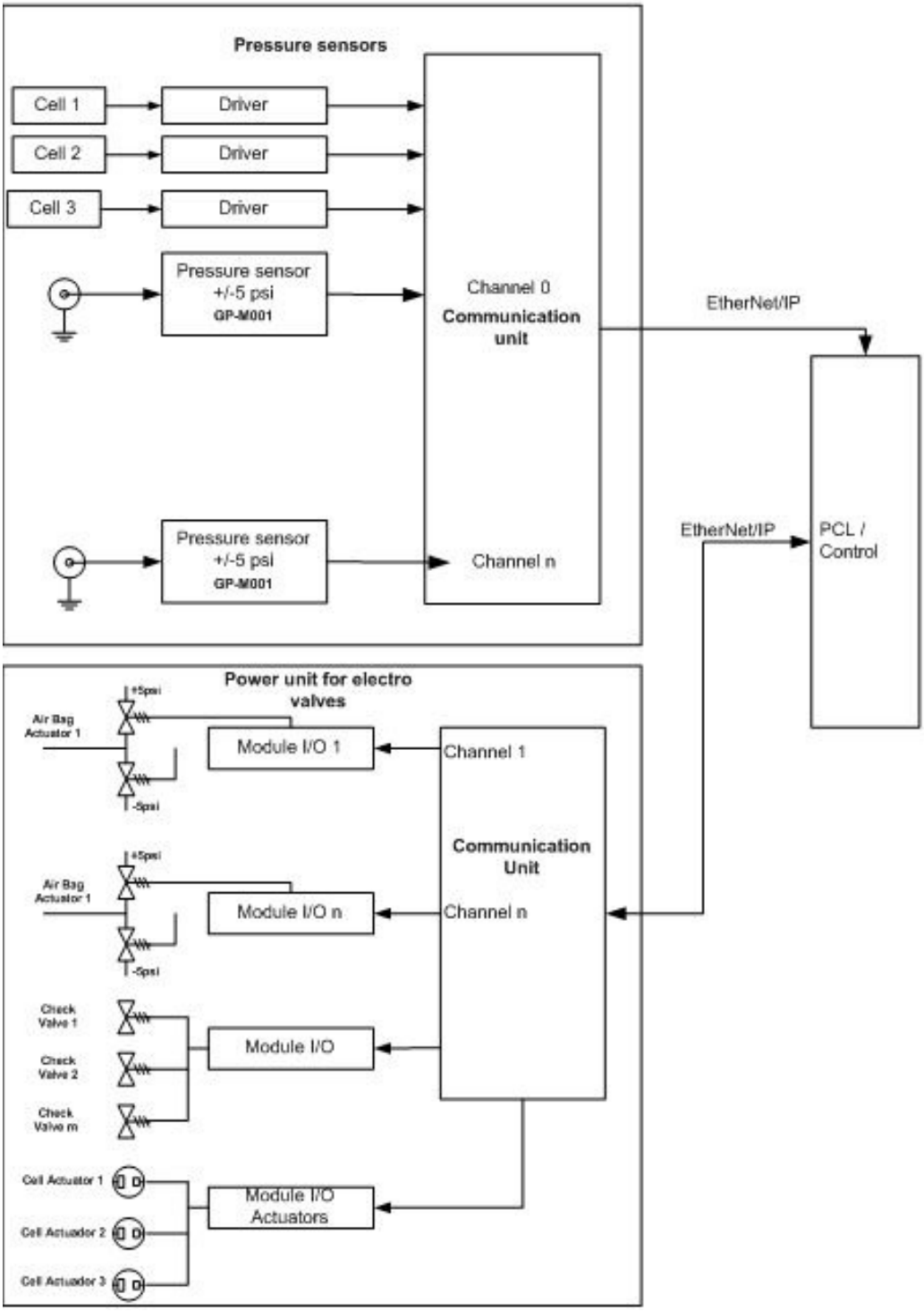

Figure 7-1. Block system diagram.

8. CONCLUSIONS

In this work the parameters of the components for the tertiary subsystem have been satisfactorily determined. The design to satisfy the parameters of each component has been developed up to 50 % in some cases, as is the case of the flexures, to 90 % like the airbag configuration, mirror and the cell design. The materials of the mirror, the cell, the hydrostatic ring and the active actuators were determined. Static analyses were made to determine the best configuration for the position of the bags. Also, the range for the working air, vacuum and hydrostatic pressure was determined.

The results obtained from the optical surface deformation of the mirror are slightly over λ/25 and are in the proper range for this optical element in the error budget. The introduction of the airbags has given good results up to this stage of the project.

The structural shape of the cell has been obtained with the main components integrated like the spherolinders [9] that are the interfaces with the tower support, the clips to secure the mirror inside the cell and the interfaces for the bag valve connectors. Static analyses were made to optimize its shape with the load it will hold. FEA static and thermal analyses of the tertiary subsystem attached to the tower system were made to obtain an approximation of the maximum travel the actuators will need to compensate for the deformations and tilts produced by the gravity and thermal loads on the system support structure. The values obtained with the configuration presented in this work, the misalignments can be compensated but the wind and seismic load analyses still need to be performed.

The contribution of the error produced by the deformation of the M3 is less than 0.04% of the total degradation of the image. This means that a contribution of 0.011 arc sec FWHM has no weight over the total error budget.

An interferometric mechanism inside the tube as feed-back for the tertiary mirror airbag control to correct the misalignment of the system produced by the flexure of the interfaces and the deformations of the optical surface is suggested.

This tertiary mirror subsystem is much simpler, smaller, lightweight and has a much lower profile than others that use counterweights or a combination of hydraulic pistons with active pneumatic actuators or spring-loaded actuators.

REFERENCES

[1] Willey, R.R. and Parks, P.E., [Opto-mechanical Engineer Handbook]. Anees Ahmad. Boca Raton: CRC Press LLC, 135-146 (1999).
[2] Magellan Project 6.5m Telescope. [Tertiary mirror cell assembly No. 96TE0500]. Magellan Observatories of the Carnagie Institution of Washington, electronic 2D drawing (1997).
[3] Magellan Project 6.5m Telescope. [Tertiary mirror No. 95TE0501]. Magellan Observatories of the Carnagie Institution of Washington, electronic 2D drawing (1997).
[4] Cavaller, L., et. All. "M3 unit preliminary mechanical design". RPT/POTI/0124-L. 2-A, 1-61 (2000).
[5] Ruiz, E. et. all. "Common-pull, multiple-push, vacuum-activated telescope mirror cell". Appl. Opt, 53(33), 7979-7984 (2014).
[6] Ruiz, E. et. All. "Celda Activa push-pull con vacio del telescopio OAN 2.1m". Publicaciones Técnicas del instituto de Astronomía. MU-2016-03, 2-6 (2016).
[7] Salas, L. G., "Active primary mirror support for the 2.1m telescope at the San Pedro Mártir Observatory". Applied Optics, 36 (16), 3708-3716 (1997).
[8] Lemaitre, G. R., "Astronomical Optics and Elasticity Theory. Active Optics Methods". France: Springer-Verlag (1st ed., Vol. 1). (2009).
[9] Spherolinder, http://www.g2-engineering.com/products-SPH
[10] Pedrayes, M. "M3 Tertiary Mirror", TSPM-OP-M3-TM, electronic drawing (2017).
[11] Pedrayes, M. "M3 Tertiary Mirror Cell", TSPM-OP-M3-TC, electronic drawing (2017).
[12] Pedrayes, M. "M3 Active System", TSPM-OP-M3-TL-SN/000, electronic drawing (2017).
[13] Pedrayes, M. "M3 Bag Support", TSPM-OP-M3-TL-TB, electronic drawing (2017).

[14] DSCR Pancake Load Cell, https://appmeas.co.uk/products/load-cells-force-sensors/low-profile-tension-compression-load-cell-dscrc/
[15] https://www.physikinstrumente.com/en/products/linear-stages-and-actuators/stages-with-motor-screw-drives/m-238-high-load-linear-actuator-with-dc-motor-703750/
[16] ULE Corning Code 7972 Ultra Low Expansion Glass, https://www.corning.com/media/worldwide/csm/documents/7972%20ULE%20Product%20Information%20Jan%202016.pdf
[17] 300 D. Cordura®. http://www.seattlefabrics.com/Cordurareg_c_78.html
[18] TSPM f/5 Nasmyth configuration design requirements, RQ/TSPM-OP/001, 1.A (2017).
[19] TSPM Coordinate Subsystem, TEC/TSPM/007, 1.F (2017).
[20] TSPM Telescope specifications, SP/TSPM-TL/001, 1.B (2017).
[21] TSPM High level Requirements, TSPM/HLREQ-001, 1.G (2017).
[22] TSPM Tertiary Mirror Assembly PD, TEC/TSPM-PDR-TL/005, 1.B, (2017).